Haloxylon salicornicum extract as an eco-friendly corrosion inhibitor for carbon steel in HCl solution

M.F. Atia,[1] A.M. Hamzah,[2] M.E. Eissa,[3] A. El-Hossiany,[4,5] and A.S. Fouda[4]*

[1]Department of Chemistry, Faculty of Science, Tanta University, Tanta, Egypt
[2]Department of Chemistry, Faculty of Science, Alexandria University, Alexandria, Egypt
[3]College of Science, Chemistry Department, Imam Mohammad Ibn Saud Islamic University (IMSIU), Riyadh 11623, KSA
[4]Department of Chemistry, Faculty of Science, Mansoura University, Mansoura-35516, Egypt
[5]Delta Fertilizers Company in Talkha, Daqahlia, Egypt
*E-mail: asfouda@hotmail.com

Abstract

The *Haloxylon salicornicum* (HS) extract ability to prevent carbon steel alloy (CS) from corroding in 1 M HCl was investigated. Research methodologies included electrochemical techniques like potentiodynamic polarization (PDP) and electrochemical impedance spectroscopy (EIS) techniques as well as chemical method like weight loss (WL). The extract provides 94.1% inhibitory efficiency (*IE*) to carbon steel (CS) submerged in a one molar HCl solution at 300 ppm, according to the gravimetric method. The inhibition efficiency of the HS extract increases with increasing the concentration and decreases with temperature, from 25 to 45°C. Polarization (PDP) study revealed that the extract was a mixed type of inhibitor. The obtained results from EIS revealed that the gradual increase in the HS concentration and time of immersion leads to progressive increase in *IE*. Impedance responses showed that the corrosion process occurred under diffusion control. The HS's adsorption adhered to the Langmuir adsorption isotherm, and the extract species' mixed kind (both physical and chemical) of adsorption on the metal surface was suggested by the adsorption's free energy. The adsorbed film on CS surface was confirmed using atomic force microscope (AFM) and X-ray photoelectron spectroscopy (XPS) techniques and was supported by electrochemical studies. Activation parameters were determined in the presence and absence of HS. Hence, HS extract has good corrosive inhibitive effect on carbon steel in HCl solution. It turned out that all methods used were consistent with one another.

1. Introduction

Natural processes such as corrosion, which can be classified as chemical or electrochemical in nature, destroy metal and alloys' metallic qualities and render them unsuitable for use in

particular applications. Metal corrosion is a serious industrial issue that has generated a lot of study and inquiry. This is because metal is more vulnerable to corrosion when exposed to hostile media (such as acid, base, or salt) due to industrial operations including acid cleaning, pickling, and etching. Several measures have been taken to lessen the threat posed by industrial facilities corroding. Nevertheless, using corrosion inhibitors is one of the greatest methods for preventing metal from corroding. In the industrial sector, corrosion inhibitors are commonly used to lower the rate at which metals and alloys corrode when exposed to harsh environments. The majority of corrosion inhibitors are costly, synthetic compounds that pose serious environmental risks. Finding corrosion inhibitors that are harmless for the environment is therefore desired [1–7]. Organic compounds with p-electrons in triple or conjugated double bonds and electronegative functional groups make up the majority of the most well-known corrosion inhibitors. The main adsorption centers for this family of inhibitors are the presence of aromatic rings and heteroatoms (such S, N, O, and P) in their structures. Numerous inhibitors have been produced and employed to prevent mild steel from corroding in acidic environments; nevertheless, several of these inhibitors pose a threat to the environment. Natural products derived from plants have been demonstrated to include a variety of organic compounds, the majority of which are known to have inhibitory effects. "These chemicals include alkaloids, tannins, pigments, and organic and amino acids". A review of the literature has revealed that the phytochemical molecules found in plants adsorb on the metal's surface [8–10], obstructing the metal's surface and preventing the corrosion process from occurring. This is the reason for the inhibitory action of some plant solutions. HS is believed to prevent corrosion because it contains molecules of arabinogalactan, oligosaccharides, polysaccharides, glycoprotein and triterpenoids [11] that contain oxygen and nitrogen atoms which considered as centers of adsorption [12]. The extract components are also thought to be the primary source of the plant's anti-inflammatory, hepatoprotective, and antioxidant properties. Green corrosion inhibitors don't include heavy metals or other harmful materials, are inexpensive, and biodegrade. Several research groups have found success using naturally occurring chemicals to avoid metal corrosion in both acidic and alkaline environments. In light of this, it has been shown that ethanol or plant-based aqueous extracts can effectively prevent some metals from corroding. Thus, the goal of this study is to find out how well ethanol extracts of HS stop CS from corroding in a 1 M hydrochloric acid solution. In addition to its many other advantageous qualities, carbon steel is used in many different sectors due to its simple availability, low cost, ease of manufacture, and strong tensile strength. When it comes into contact with acid solutions during chemical procedures such as de-scaling, acid storage, acid cleaning, and acid transportation, it corrodes severely. Currently, industry uses some organic compounds as corrosion inhibitors to stop or slow down metal corrosion in acidic solutions. These compounds are expensive and hazardous, thus it's important to find less expensive and ecologically acceptable inhibitors [13–16]. HS, a member of the *Amaranthaceae* family of plants, has therapeutic use. This shrub is native to the desert and may be found in the following countries: Afghanistan, Pakistan, Saudi Arabia, Kuwait, Oman, Israel, Jordan, and Egypt. It is an almost leafless shrub that branches to a maximum height of

60 cm. The plant has pale stalks with small triangular cup-shaped scales that have fuzzy interiors and membrane edges, but it lacks wide foliage-type leaves. Blooms are produced on short spikes up to 6 cm long. This plant grows on sand dunes, sandhills, and other arid places with huge, spreading shrub with irregularly angled glabrous branches. The blossoms have a vivid yellow hue. This plant has a large number of beneficial chemical components. HS has a wide range of therapeutic uses, including antibacterial, antioxidant, antidiabetic, antiulcer, anthelmintic, anticancer, and assistance with liver damage [17–21].

Table 1 shows how several authors used herbal extracts as inhibitors to reduce metal corrosion in a variety of common industrial solutions [22–30].

Table 1. List of plant sources utilized for dissolution inhibition studies.

Plant	Metal*	Corrosive medium	%IE	Ref.
Bacopa monnieri	LCS	0.5 M NaOH	80.0	[22]
Camellia sineniss	CS	3.5% NaCl	80.0	[23]
Dioscorea septemloba	CS	1 M HCl	72.0	[24]
Euphorbina heterophylla llinneo	MS	1.5 M HCl	69.0	[25]
Ipomoea batatas	GS	1 M HCl	64.0	[26]
Cola acuminata extract	LCS	1 M HCl	74.0	[27]
Admixture of rosemary and cinnamon cassia oil	MS	0.5 M H_2SO_4 and HCl	99.21, 97.69	[28]
Orange pee	Mg	NaCl	85.7	[29]
Rosemary and myrtle	Cu	NaCl	92.5	[30]
Harmal leaves	CS	0.25 M H_2SO_4	98.0	[31]
Mikania micrantha	1060 Al	1 M HCl	97.0–93.6	[32]
Chromolaena Odorata leaf	MS	1 M HCl	83.3	[33]

*LCS = low carbon steel, CS = carbon steel, MS = mild steel, GS = galvanized steel.
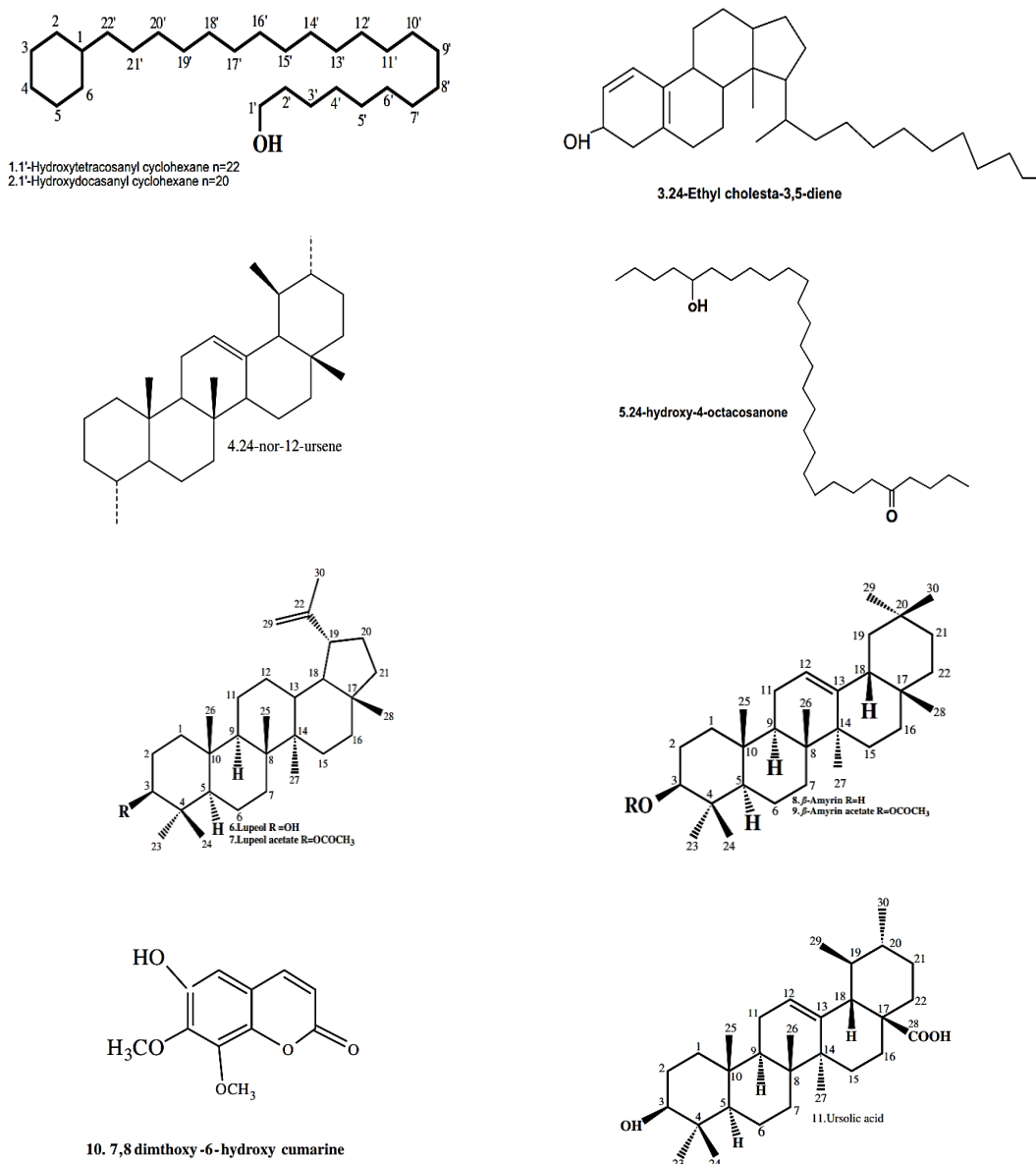
In this work, potentiodynamic polarization, electrochemical impedance spectroscopy (EIS) and gravimetric methods were used to examine the adsorption and corrosion inhibition effect of HS extract in one molar HCl. The surface morphology of the CS samples was tested using different techniques.

2. Experimental Measurements

2.1. Materials and solutions

For every experiment an acidic medium (1 M HCl) was created by diluting analytical grade HCl reagent (37%) with double-distilled water. CS composition (in weight %) is C = 0.2, Mn = 0.37, P = 0.026, Si = 0.002, and Fe is the balance. The CS samples were polished using

various emery sheets ranging in grade from 400 to 1200. After that, they were cleaned with acetone and allowed to dry at room temperature. After being gathered, the HS was dried, chopped into small pieces, and then dried for 72 hours in the shade before being milled into a powder. In a Soxhlet system, 10 g of dry powder was extracted with methanol for three hours. It was discovered that the extract's concentration ranged from 50 to 300 ppm. The fragments of HS that had just been harvested were first dried and pounded into a powder. Once the extraction process was finished, the extract was filtered and boiled to 55°C in a water bath until the majority of the methanol evaporated. The inhibitor test solutions with concentrations ranging from 50 to 300 ppm were made from the stock solution (1 g/L) by diluting with doubly distilled water. Chromatographic separation of HS extract's primary constituents is depicted in Figure 1 [34].
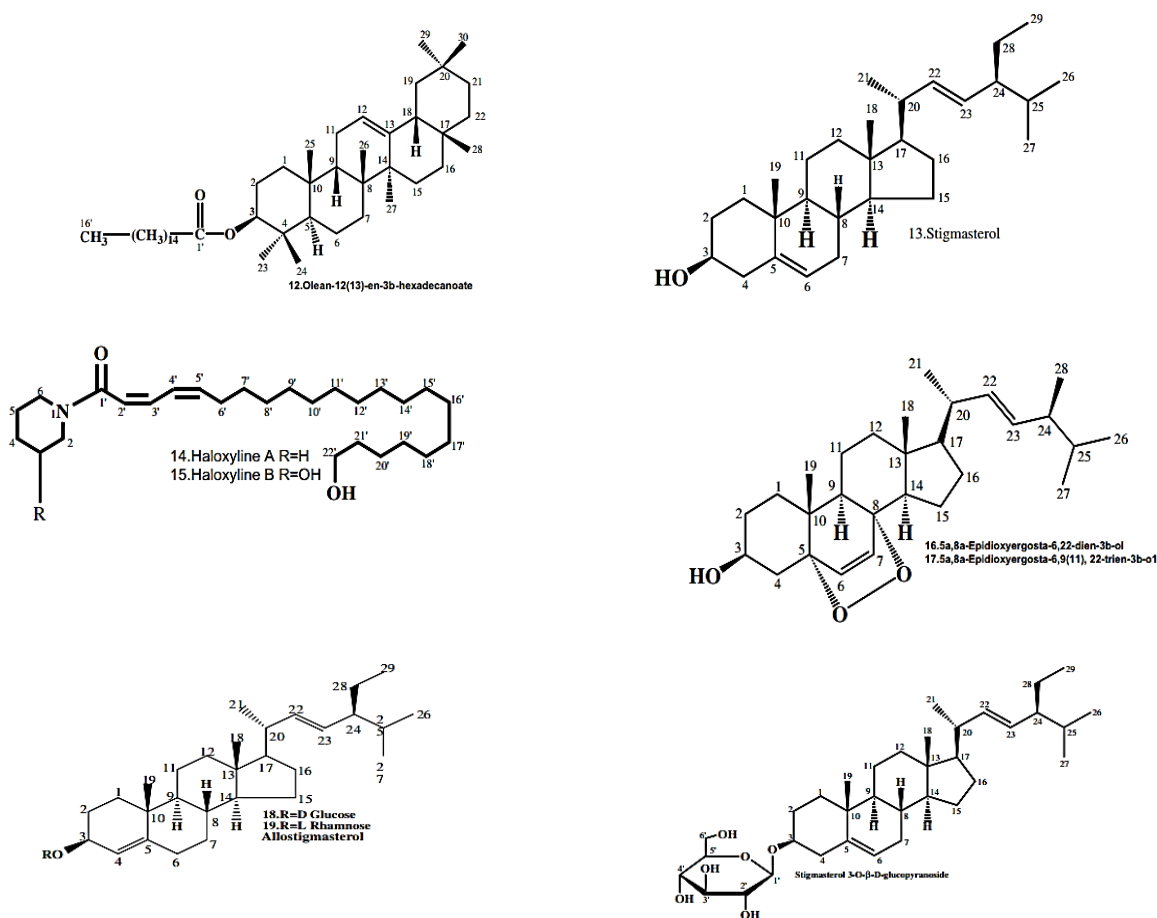

1.1'-Hydroxytetracosanyl cyclohexane n=22
2.1'-Hydroxydocasanyl cyclohexane n=20

3.24-Ethyl cholesta-3,5-diene

4.24-nor-12-ursene

5.24-hydroxy-4-octacosanone

6.Lupeol R =OH
7.Lupeol acetate R=OCOCH₃

8. β-Amyrin R=H
9. β-Amyrin acetate R=OCOCH₃

10. 7,8 dimthoxy -6- hydroxy cumarine

11.Ursolic acid

Figure 1. Main components in the *Haloxylon salicornicum* plant.

2.2. Weight loss (WL) method

After precisely weighing and preparing carbon steel $2\times2\times0.2$ cm, the samples were placed in 100 mL solutions of an acidic corrosive medium with varying concentrations of HS extract (50, 100, 150, 200, 250, and 300 ppm) and allowed to dip for 30, 60, 90, 120, 150, and 180 minutes. It is possible to compute the corrosion rate (*CR*) as follows:

$$CR = \Delta W / At \qquad (1)$$

where ΔW is WL (mg), A is the surface area of the CS parts in cm^2 and t is the engagement time in minutes.

2.3. Electrochemical tests

A three-electrode glass cell including a working electrode which made from CS sheet insulated with araldite with one cm^2 area, a reference electrode (SCE), and an auxiliary electrode (Pt) was used for the electrochemical measurements. In order to achieve a stable state, the electrode was submerged in the test solution at open circuit potential (OCP) for 30 min prior to measurement. Curves of PDP were recorded between -500 and $+500$ mV$_{SCE}$ against OCP at a scan rate of 0.2 mV·s^{-1}. Each test was performed on a freshly cleaned

electrode utilizing a freshly prepared electrolyte. Measurements were made of the corrosion parameters, including the Tafel slopes (β_c and β_a,), corrosion potential E_{corr}, and corrosion current density i_{corr}. Using a three-electrode cell assembly, AC impedance spectra were collected in the same apparatus for polarization research. For a range of frequencies, the real and imaginary parts of the cell impedance were measured in ohms. The values of the double-layer capacitance (C_{dl}) and charge transfer resistance (R_{ct}) were calculated. EIS measurements were carried out in the frequency range of 50 kHz to 0.1 Hz with amplitude of 10 mV peak-to-peak. All the electrochemical tests were carried out at 25°C. %IE and θ were determined from chemical and electrochemical measurements" as shown in Table 2.

Table 2. Equations to determine the %IE.

Technique	Equation	
WL [35]	$\% IE = \left[1-\left(W_i/W_0\right)\right]\cdot 100$	(2)
PDP [36]	$\% IE = \left[1-\left(i_{corr}/i_{corr}^0\right)\right]\cdot 100$	(3)
EIS [37]	$\% IE = \left[1-\left(R_{ct}^0/R_{ct}\right)\right]\cdot 100\%$	(4)

where W_0 weight of the samples without HS extract; W_i is the weight of the samples with HS extract; i_{corr} is the current density in the presence and absence of extract; while R_{ct}^0 and R_{ct} are the data of resistance in the absence and presence of HS extract, correspondingly. At least three replications of each experiment were conducted in order to assess reproducibility.

2.4. Surface analysis

The morphology of the CS surface was examined using AFM and XPS before and after 24 hours of immersion in a corrosive acidic environment without and with 300 ppm (highest dose) HS. Atomic force microscopy is an effective method for studying the surface morphology of CS alloys at the Nano or micro scale. Electronic X-ray spectroscopy (XPS) measurements were carried out using an ESCALAB 250Xi, Thermo-Scientific, USA [38].

3. Results and Discussion

3.1. Gravimetric method

The rate at which a metal (CS) dissolves in solution describes its corrosion behavior in an aqueous environment. The test environment's corrosiveness and the rate at which material loss from corrosion happens are both determined by corrosion rate measurements [39, 40]. The traditional method for evaluating corrosion rates is the gravimetric test. This method precisely evaluates the ability of HS to protect surface of CS from corrosion. Optimizing the usage of the inhibitor becomes simple with this procedure. This method has proven to be the most accurate method for determining inhibitor effectiveness (%IE) and corrosion rate (CR).
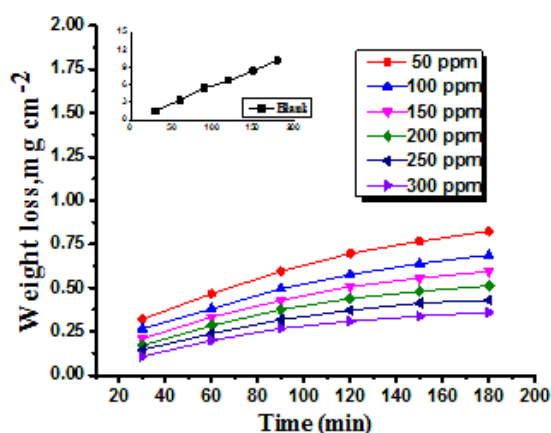
Figure 2. WL–time curves for the dissolution of CS in 1 M HCl in the presence and absence of altered doses of *HS* extract at temperature of 25°C.

Table 3. *CR*, θ and %*IE* for various doses of HS at 25°C.

Conc., ppm	$CR \cdot 10^4$, mg·cm^{-2}·min^{-1}	θ	%*IE*
Blank	630	–	–
50	67	0.894	89.4
100	57	0.910	91.0
150	52	0.917	91.7
200	46	0.927	92.7
250	40	0.937	93.7
300	37	0.941	94.1

The WL test is usually selected since the quantity calculated is directly related to the precision level. In HCl acid that is both uncontrolled and inhibited, the linear relation of WL with time (Figure 2) shows that there are no insoluble surfaces layers caused by corrosion, where the HS is first adsorbed on the surface of the CS alloy and then reduced the *CR* and hence increase the %*IE*. Table 3 shows that the maximum %*IE* of 94.1% was reached at 300 ppm. and that increasing the extract's concentration further did not significantly alter the %*IE*'s performance. The validation was that the concentration achieved the whole surface covering, and any additional after that did not result in a rise in the percentage of *IE* [41].

3.2. Temperature effect

WL experiments were utilized to examine the effects of temperature on *CR* and %*IE* of CS in HCl with and without doses of HS in the temperature range (from 25 to 45°C) and results obtained are given in Table 4. The *CR* rose and the extract's percentage *IE* dropped as the temperature rose (Table 4). The explanation for this was that a temperature rise impacted the

adsorption/desorption ratio rate. As desorption occurred more quickly than adsorption, the percentage of *IE* decreased as a result [42]. The activation energy of the corrosion process in the presence of extract was often enhanced by the drop in %*IE* with an increase in temperature [43, 44].

Table 4. The results of WL technique (*CR*, θ and %*IE*) for CS in the presence and absence of HS extract after 120 min, at (30, 35°C).

Conc., ppm	30°C		35°C		40°C		45°C	
	CR	*%IE*	*CR*	*%IE*	*CR*	*%IE*	*CR*	*%IE*
Blank	0.082	–	0.1130	–	0.1550	–	0.1730	–
50	0.0088	88.0	0.0148	86.0	0.0230	84.5	0.0305	82.4
100	0.0081	88.9	0.0135	87.2	0.0204	86.2	0.0277	84.0
150	0.0073	89.9	0.0119	88.6	0.0185	87.4	0.0266	84.6
200	0.0064	91.0	0.0103	90.0	0.0172	88.3	0.0241	86.1
250	0.0057	91.8	0.0092	91.0	0.0151	89.6	0.0212	87.7
300	0.0046	93.2	0.0078	92.2	0.0121	91.5	0.0174	89.9

The estimates of E_a^* for corrosion of CS in uninhibited and inhibited acid corrosive medium were computed by employing Arrhenius expression [45]:

$$\log CR = -E_a^*/2.303RT + \log A \tag{5}$$

where *A* is the pre-exponential Arrhenius multiplier. Straight lines were achieved by drawing log *CR* versus 1/*T* without HS and at different doses of HS (Figure 3) with a slope of ($-E_a^*/2.303R$). The entropy (ΔS^*) and enthalpy (ΔH^*) of the CS corrosion process in an aggressive acidic environment in the absence and presence of altered doses of HS were calculated using next Equation [46]:

$$CR = RT/Nh \cdot \exp^{(\Delta S^*/R)} \cdot \exp^{\left(-\Delta H^*/RT\right)} \tag{6}$$

where *h* represents Planck's constant. Plotting log *CR*/*T vs.* 1/*T* with and without an adjusted dose of HS yielded straight lines (Figure 4). Table 6 displays the highest values of E_a^* and ΔH^* when HS is absent, suggesting that chemical adsorption of *Haloxylon salicornicum* takes place on the CS surface. Positive values for ΔH^* indicate endothermic adsorption of HS molecules on the CS. A negative ΔS^* value means that the extract transfers the reactants to the active compound by reducing them [47, 48].
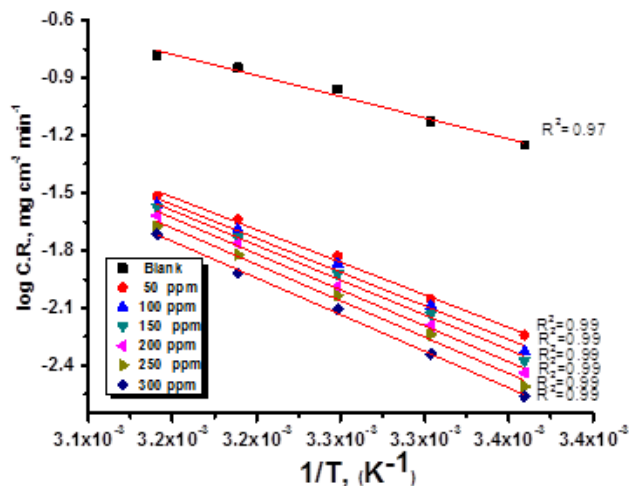
Figure 3. Plotting log *CR* versus 1/*T* for CS in the presence and absence of altered doses of HS extract.
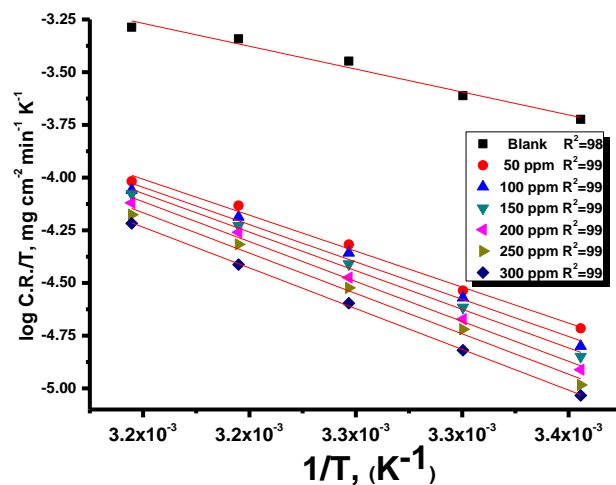

Figure 4. Plotting log *CR*/*T* against 1/*T* for CS in the presence and absence of various doses of HS extract.

Table 6. E_a^*, ΔH^*, and ΔS^* for CS in the presence and absence of various doses of HS extract.

C_{inh}, ppm	E_a^*, kJ/mol	ΔH^*, kJ/mol	$-\Delta S^*$, J/mol·K
Blank	38.5	35.9	122.8
50	61.2	58.6	62.0
100	63.5	60.9	55.2
150	65.7	63.1	48.3
200	68.0	65.4	41.6
250	68.8	66.2	40.1
300	69.5	66.9	39.2

3.3. Adsorption isotherm

The interactions between the extract components and the metal surface, which contains active sites, are described by the adsorption isotherm. One of the well-known adsorption isotherm models may be used to determine the effectiveness of the adsorbent type of examined HS by fitting the experimental results. The isotherm is determined using the linear relationship between the concentration of the HS extract (C) and the degree of surface coverage (θ) values ($\theta = \%IE/100$). Various adsorption isotherms, including kinetic-thermodynamic, Temkin, Henry, and Langmuir and Frumkin isotherms, were applied. A model which is having highest R^2 is the most excellent model to get information about the performance of adsorption-type inhibitor. It was determined that the Langmuir adsorption isotherm provided the best fit (high $R^2 > 0.999$). Figure 5 shows the representation of the Langmuir for HS extract. This isotherm accurately describes the relationship between adsorption and concentration. As in Equation 7:

$$C/\theta = 1/K_{ads} + C \tag{7}$$

Within the given context, the HS concentration (measured in ppm) inside the bulk electrolyte is indicated as C, and the surface coverage degree (θ). The adsorption constant is recognized as K_{ads}. Plotting C/θ *vs.* C further demonstrated the validity of the Langmuir adsorption isotherm, with the intercept being found to be $1/K_{ads}$, however the values of the slopes deviate significantly from the unity. This deviation in slope values may be due to the interactions between adsorbate molecules in adjacent active sites that were ignored by the Langmuir equation for adsorption isotherm [49, 50]. By utilizing Equation 7, The values of (K_{ads}) were determined. The adsorption constant, K_{ads}, gained from the equation of the Langmuir adsorption isotherm, is specifically related to the free energy of adsorption, ΔG^0_{ads} by the relation:

$$\Delta G^0_{ads} = -RT \ln(55.5 \cdot K_{ads}) \tag{8}$$

The numerical value 55.5 corresponds to the solution's water molarity, indicating the number of moles of water per liter. Table 7 depicts the parameters of the adsorption of the obtained HS extract. As the achieved negative values of ΔG^0_{ads} decrease with increasing temperature, indicating greater stability of the adsorbed layer at low temperature, and the spontaneous process of the adsorption of the extract on the surface of the CS alloy. Generally speaking, ΔG^0_{ads} values up to -20 kJ/mol are indicative of physical adsorption with the electrostatic interaction between charged molecules and the charged metal, while values more negative than -40 kJ/mol indicate chemisorption or the sharing or transfer of electrons from the inhibitor molecules to the metal surface to form a coordinate type of bond [51]. The ΔG^0_{ads} values in the current investigation were between 20–40 kJ/mol indicating the HS molecules were adsorbed on the metal surface physically and chemically [52, 53] and due to the increase in E^*_a in presence of extract than in its absence and the decrease in $\%IE$ with

rise in temperature, the adsorption of HS on CS surface is mainly physical [54]. The enthalpy of adsorption (ΔH_{ads}^0) was computed utilizing the following Vant Hoff Equation:

$$\log K_{ads} = -\Delta H_{ads}^0 / 2.303RT + \text{constant} \tag{9}$$

Plotting $\log K_{ads}$ versus $1/T$ produces a straight line as shown in Figure 6. The adsorption entropy (ΔS_{ads}^0) can be calculated as follows:

$$\Delta G_{ads}^0 = \Delta H_{ads}^0 - T\Delta S_{ads}^0 \tag{10}$$

Table 7 displays the computed ΔH_{ads}^0 and ΔS_{ads}^0 values. The negative sign of ΔS_{ads}^0 indicates the increased ordering of HS molecules upon adsorption onto the metal surface [55].
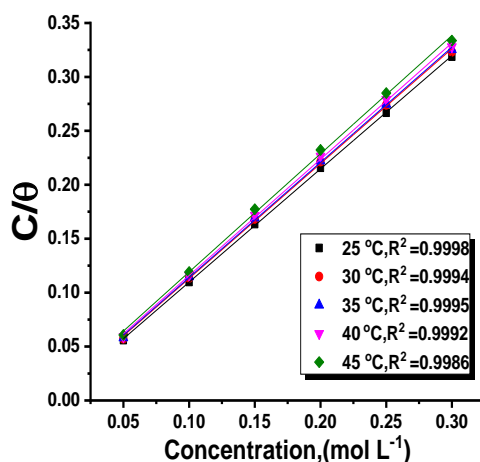
Figure 5. Langmuir's adsorption isotherm plots for CS in 1 M HCl containing various doses of HS extract.

Table 7. Langmuir parameters for the adsorption of HS extract on the CS surface at varied temperatures.

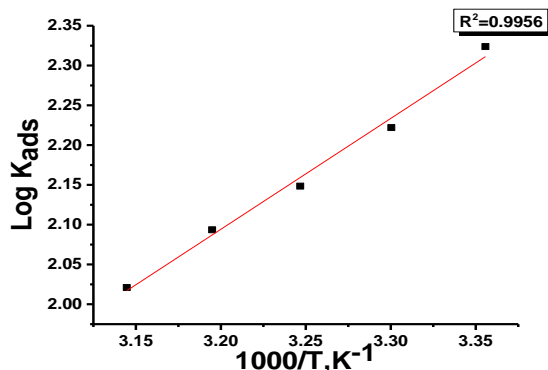| T, K	K_{ads}, mol/l	$-\Delta G_{ads}^0$, kJ/mol	$-\Delta H_{ads}^0$, kJ/mol	$-\Delta S_{ads}^0$, J/mol·K
298	211	23.2		77.8
303	161	22.9		75.5
308	136	22.8	26.0	74.2
313	113	22.7		72.6
318	96	22.6		71.3

Figure 6. Effect of altered temperatures on the free energies of Langmuir isotherms.

3.4. PDP tests

Predicting the type of inhibitor and identifying the best mechanism for the inhibition process are accomplished by electrochemical investigations. Figure 7 illustrates the PDP curves at various concentrations of extract. Table 8 depicted the polarization parameters of the PDP test: corrosion potential (E_{corr}), corrosion current density (i_{corr}), anodic Tafel (β_a), cathodic Tafel (β_c), slopes CR, θ and $\%IE$. The values of E_{corr} in the Table showed that the extract caused the potential to shift towards positive values. The potential shifts were observed to vary by a maximum of 20 mV (less than 85 mV) towards both negative and positive values, indicating that HS extract acted as mixed-type inhibitor [56, 57]. The corrosion current density (i_{corr}) was determined by finding the intersection of the cathodic and anodic Tafel lines. The value of i_{corr} reduced as the concentration of extract increased, leading to a comparable increase in $\%IE$. This suggested that the extract could reduce CS corrosion in 1 M HCl medium [58, 59]. The values of β_a and β_c were not significantly altered by the increase the extract concentration when compared to the absence of extract. This means that the mechanism of cathodic and anodic reactions was not changed in the presence of the extract. The parallel Tafel lines indicated that the corrosion mechanism of CS was unaffected by its presence or absence.

Table 8. Calculations of corrosion parameters for CS in 1.0 M HCl with altered inhibitor doses.

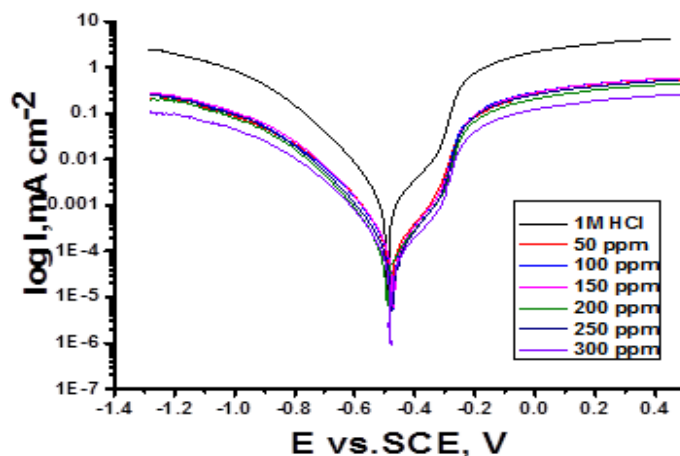| Conc., ppm	i_{corr}, µA/cm²	$-E_{corr}$, mV *vs.* SCE	β_a, mV/dec	$-\beta_c$, mV/dec	CR, mm/y	θ	$\%IE$
Blank	482	491	108	127	218	–	–
50	151	513	118	142	98	0.687	68.7
100	115	511	115	134	72	0.761	76.1
150	98	510	118	137	58	0.797	79.7
200	76	504	114	138	54	0.841	84.1
250	59	503	99	131	35	0.877	87.7
300	41	501	106	129	27	0.915	91.5

Figure 7. An illustration of the PDP curves that show the dissolving behavior of CS when HS extract are present and absent at 25°C.

3.5. EIS test

For the analysis of electrochemical systems, electrochemical impedance spectroscopy (EIS) stands out as one of the most useful techniques (EIS). The Nyquist and Bode plots are shown in Figures 8 and 9, respectively. A charge transfer process is implied by the half-loop Nyquist curves of the studied system with one time constant. Blank loops have a smaller diameter than inhibitor loops, and loop forms are not altered as inhibitor concentration increases. According to these results, the corrosion process is not changed, and a covering film may form on the surface of the CS due to adsorption of the extract [60]. Thus, corrosion reaction is governed by the process of charge transfer between metal and solution [61]. The electrode surface may be protected from acidic solution by an adsorbed inhibitor film HS extract, which reduces contact with the acidic environment and inhibits CS dissolution. An evident time constant is detected in the Bode plots Figure 9. The only one peak observed in Bode plots for the extract manifested the presence of single time constant as mentioned in Nyquist plot. A frequency dispersion induced deviation has been avoided by replacing the ideal capacitance of double layer (C_{dl}) with the CPE in the equivalent circuit". This formula defines the CPE parameter as the flattened nature of Nyquist spectra allows us to have a more precise fit [62].

$$C_{dl} = Y_0 \left(\omega_{max} \right)^{n-1} \tag{11}$$

where Y_0 is the size of the CPE, n is the CPE parameter which characterizes the deviation of the system from ideal capacitive behavior. The value of n is between -1 and 1, ω is the angular frequency ($\omega_{max} = 2\pi f_{max}$), f_{max} is the maximum frequency. CPE in Figure 10 explains the circuit components based on the value n. Thus, for exponent value n equal to 1, 0, 0.5, or 1, the following values are given: inductance, resistance, and Warburg impedance. The CPE is inserted to substitute a double layer capacitance (C_{dl}) to provide a more precise fit. In uninhibited and inhibited solutions, the R_{ct} can be used to calculate HS extract inhibition

efficiency. Table 9 displays the values of the EIS's fitted parameters. The addition of HS extract revealed an increase in charge transfer resistance (R_{ct}) by increasing the diameter in Nyquist plot [59]. Since the reference electrolyte's Y_0 value is higher than the inhibited electrolyte's, it is possible that the extract molecules interacted with the electrode surface, preventing the dissolution of the electrode surface. The (C_{dl}) dropped while the (R_{ct}) rose with the extract's concentration. The obtained data indicated that the extract molecules were adsorbed on the CS-solution interface due to a decrease in the local dielectric constant and an increase in the electrical double layer's thickness [63]. The chi-squared was utilized to appraise the precision of the fitting results, the small chi-squared values (Table 9) acquired for all the results showed that the fitted results have a great concurrence with the experimental findings. The results from the WL PDP measurements are agreed well with the results obtained from EIS tests.
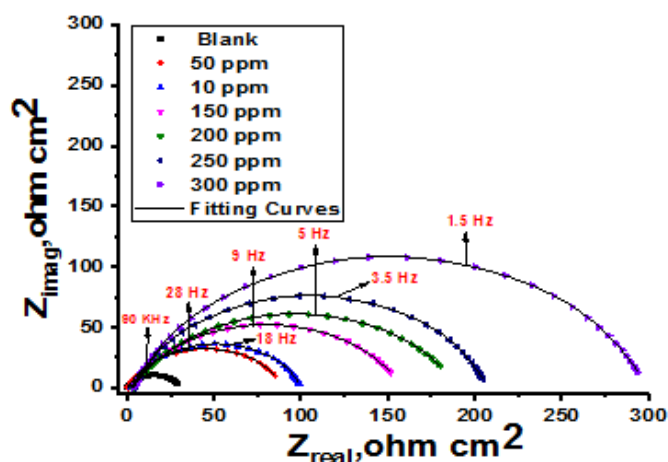
Figure 8. The Nyquist plots for CS corrosion in one molar HCl with and without altered doses of HS extract at 25°C.
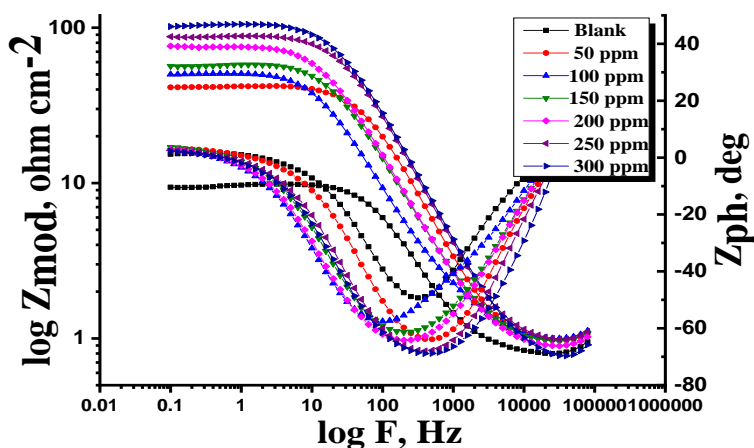
Figure 9. The Bode plots for CS corrosion in one molar HCl with and without altered doses of HS extract at 25°C.
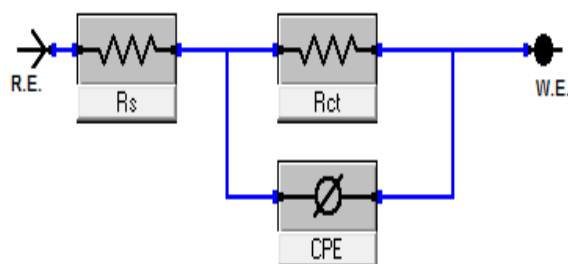
Figure 10. Electrical circuit for experimental data fitting.

Table 9. Impedance parameters for CS after immersion in one molar HCl with and without altered HS extract doses at 25°C.

Conc., ppm	Y_0, $(\mu \cdot \Omega^{-1} \cdot s^n \cdot cm^{-2}) \cdot 10^{-6}$	n	R_{ct}, $\Omega \cdot cm^2$	C_{dl}, $\mu F/cm$	θ	*%IE*
1 M HCl	262	0.859	30.23	118	–	–
50	231	0.831	84.15	103	0.641	64.1
100	227	0.819	99.98	98	0.698	69.8
150	212	0.810	151.7	94	0.801	80.1
200	209	0.785	182.7	85	0.835	83.5
250	198	0.767	210.1	75	0.856	85.6
300	177	0.756	310.9	69	0.903	90.3

3.6. Surface analysis

3.6.1. AFM studies

After dipping in 1 M HCl with 300 ppm *HS* extract and a 24-hour immersion, the surface morphology of the CS was examined using AFM experiments and was quantified in terms of surface roughness. The mean values of the "R_a" roughness profile are important for identifying and summarizing a test inhibitor's efficacy [64]. Among other things, roughness plays a role in explaining the nature of the layer adsorbed on CS. Figure 11 a, b shows the three-dimensional AFM images of abraded CS in 1 M HCl without and with 300 ppm extract, respectively. The average roughness value for abraded CS is ($R_a = 643$ nm), while for the inhibited CS is ($R_a = 133$ nm). The decrease in the roughness is due to the adsorption of the extract molecules on the CS surface. It can be said that a protective layer is formed on the surface of CS.
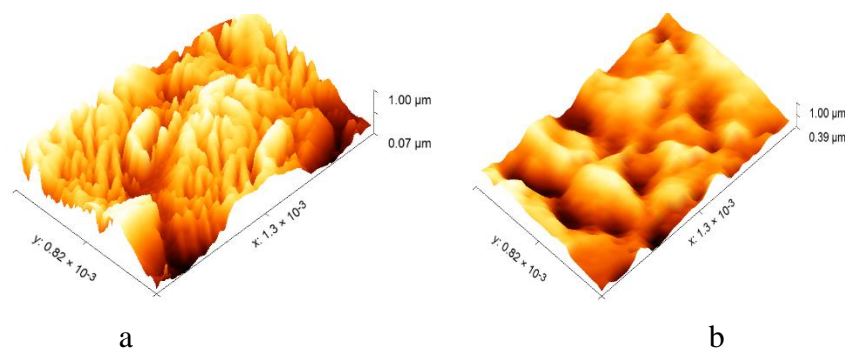
Figure 11. (a) AFM of CS specimen in 1 M HCl Only and (b) AFM of CS specimen + 1 M HCl + 300 ppm of HS extract for 24 h.

3.6.2. XPS analysis

The adsorption capacity of the HS extract is demonstrated by the CS metal's surface inhibitory layer in 1 M HCl. The XPS decomposition spectra of each element, which is present on the surface layer created in a solution that contains the extracted HS, are displayed separately in Figure 12. XPS, Fe2p, O1s, C1s and Cl2p for CS at 1 M HCl with 300 ppm from HS extract

Table 10 displays the binding energies data (BE, eV) and each peak component's identical assignment [65, 66]. The Fe 2p spectrum demonstrated at a binding energy (BE) of five peaks 710.59, 714.41, 718.34 and 724.07 eV may be ascribed to Fe_2O_3, $FeCl_3$, $FeOOH$, and Fe_3O_4 respectively. The spectrum of O 1s consists of two peaks 531.87 and 530.03 eV which at 531.87 appointed to Fe_2O_3, at 530.03 eV binding energy which associated to $Fe(OH)_3$ bond (hydroxide). The Cl 2p includes two peaks situated at 198.81 eV for Cl 2p3/2 and 201.32 eV for Cl 2p1/2. The C1s spectra represented three peaks found at 285.17, 286.91, 288.34 eV. The greatest peak at 285.17 can be ascribed to the C–C, C–H, C=C bonds of aromatic rings. Additionally, the peaks placed at 286.91 eV are ascribed to the C–O–C, C–OH bonds, individually. The peak found at 288.34 eV which attributed to O–C=O, C=O appear that the molecules of HS extract have been arranged and adsorbed on the surface of CS.

Table 10. Binding energies (BE) for the great core lines observed for the surface of CS which holds the HS extract.

Core element	BE, eV	Assignments
C1s	285.17	C–C, –C=O, C–H
	286.91	C–O–C, C–OH
	288.34	O–C=O, C=O
O1s	531.87	Fe_2O_3
	530.03	$Fe(OH)_3$

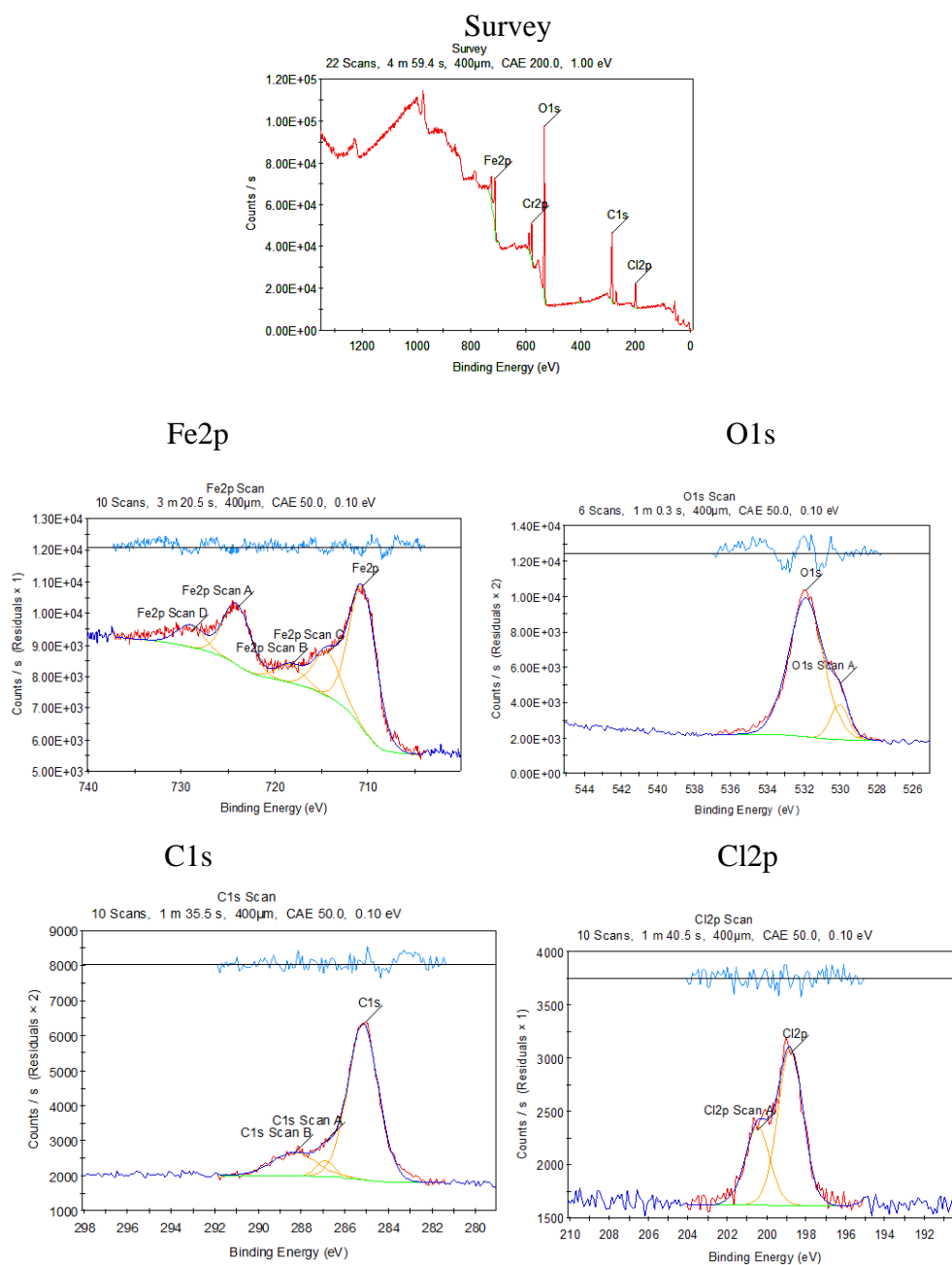| Core element	BE, eV	Assignments
Fe2p	710.59	Fe_2O_3
	714.41	$FeCl_3$
	718.34	FeOOH
	724.07	Fe_3O_4
Cl2p	198.81	Cl 2p3/2
	201.32	Cl 2p1/2

Figure 12. XPS, Fe2p, O 1s, C1s and Cl2p for CS at 1 M HCl with 300 ppm from HS extract.

3.7. Mechanism of corrosion inhibition

The adsorption process is influenced by various factors, including the interaction between CS and the solution, the electrochemical potential, the chemical composition, and the surface properties of CS. One or more of the following theories can account for the inhibitory mechanism observed in this study, which is based on the adsorption of several novel heterocyclic derivatives on the CS surface in a single molar HCl solution. One possibility is that the inhibitor molecules are chemically adsorbed on the steel surface through the donor-acceptor interaction of the unshared pair of electrons found in the substituted heteroatoms, such as N, O, and S, or through the charge-transfer interaction of the π-electron of the benzene ring to the empty low-energy d-orbital of Fe surface (anodic area). As a result, coordinate chemical bonds may form between the extract molecules and the surface of Fe^{2+}) Adsorption occurs physically when positively charged (protonated) inhibitor molecules form an electrostatic attraction with negatively charged chloride anions adsorbed on the iron surface ($FeCl^-$) which acts as a bridge between the inhibitor molecules and the steel surface. Alternatively, protonated inhibitor molecules may adsorb on the cathodic region and compete with hydrogen ions for adsorption, which increases the activation of cathode polarization [67]. Combining the π-electron and electrostatic interactions is an additional possibility [68]. The second possibility is strongly supported by several experimental observations. Initially, the inhibitor molecules readily protonate in HCl solution to form positively charged inhibitor species. The surface charge of the CS at zero, or the so-called zero charge potential (ZCP), has to be determined. This can be computed using the formula ($E_{corr} - E_q = 0$). The surface charge is positive when ($E_{corr} - E_{q=0}$) > 0 [69]. According to measurements made previously [70], the ZCP of iron in HCl solution is $E_q = -530$ mV *vs.* SCE. Referring back to Table 8's findings, the extract in one molar HCl had a maximum E_{corr} value of 513 mV *vs.* SCE at 300 ppm. As a result, the matching Fe-ZCP computed value is 17 mV, indicating that the CS surface is positively charged. Therefore, it is anticipated that there will be electrostatic repulsion between the positively charged steel surface and the protonated charged extract molecules. However, because of the electrostatic interaction between the anionic species and the protonated charged extract molecules on the electrolyte/metal interface, it is also anticipated that the surface of the CS will be covered with negatively charged chloride ions (Cl^-) in the HCl solution. As a result, the first adsorption layer is formed when the positively charged extract molecules are bound to the CS surface via the chloride-bridge. In this manner, the extract is physically adsorbed into the metal surface, resulting in the creation of a thin protective coating that drastically lowers the rate of corrosion of the CS. Because this HS is protonated, it can directly adsorb on the negative CS surface through electrostatic attraction in an acidic environment, as seen below:

Int. J. Corros. Scale Inhib., 2024, **13**, no. 2, 750–774

768
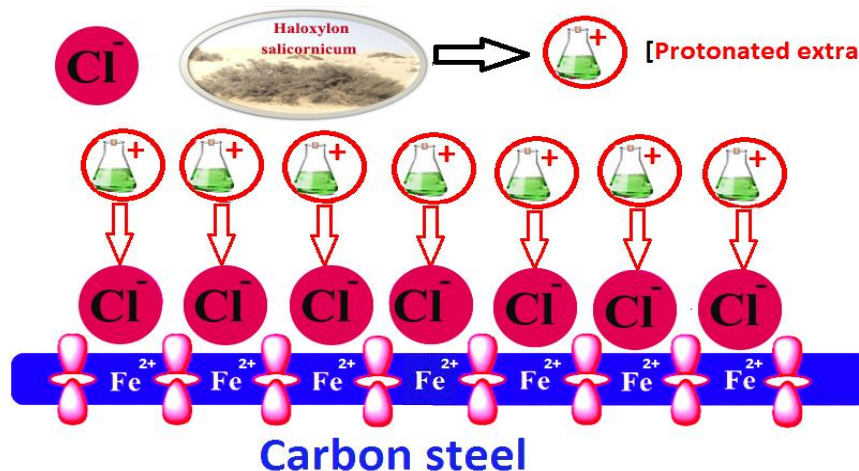
4. Conclusions

1. This work evaluated the inhibitory action of HS extracts for CS in HCl solution utilizing WL test, PDP and EIS techniques.
2. The PDP experiments indicated that HS extract was successful in preventing the corrosion of CS in HCl solution and acted as inhibitor with mixed characteristics.
3. The EIS data showed that the presence of this HS extract led to an increase in charge transfer resistance (R_{ct}) and a decrease in capacitance double layer (C_{dl}).
4. The inhibition mechanism was identified as the adsorption process, which was further supported by the Langmuir isotherm model for HS.
5. The adsorbed protective film of HS was detected by AFM and X-ray photoelectron spectroscopy techniques.

References

1. N.A. Negm, M.A. Yousef and S.M. Tawfik, Impact of synthesized and natural compounds in corrosion inhibition of carbon steel and aluminium in acidic media, *Recent Pat. Corros. Sci.*, 2013, **3**, 58–68. doi: [10.2174/2210683911303010007](#)
2. I.B. Obot and N.O. Obi-Egbedi, Ginseng root: a new efficient and effective eco-friendly corrosion inhibitor for aluminium alloy of type AA 1060 in hydrochloric acid solution, *Int. J. Electrochem. Sci.*, 2009, **4**, 1277–1288. doi: [10.1016/S1452-3981(23)15221-7](#)
3. D.-J. Choi, S.-J. You and J.-G. Kim, Development of an environmentally safe corrosion, scale, and microorganism inhibitor for open recirculating cooling systems, *Mater. Sci. Eng. A*, 2002, **335**, 228–235. doi: [10.1016/S0921-5093(01)01928-1](#)
4. B.E. Rani and B.B.J. Basu, Green inhibitors for corrosion protection of metals and alloys: an overview, *Int. J. Corros.*, 2012, **2012**, 380217. doi: [10.1155/2012/380217](#)
5. P.C. Okafor, V.I. Osabor and E.E. Ebenso, Eco-friendly corrosion inhibitors: inhibitive action of ethanol extracts of Garcinia kola for the corrosion of mild steel in H_2SO_4 solutions, *Pigm. Resin Technol.*, 2007, **36**, 299–305. doi: [10.1108/03699420710820414](#)

6. P. Muthukrishnan, B. Jeyaprabha and P. Prakash, Corrosion inhibition and adsorption behavior of *Setaria verticillata* leaf extract in 1 M sulphuric acid, *J. Mater. Eng. Perform.*, 2013, **22**, 3792–3800. doi: 10.1007/s11665-013-0700-2

7. A.S. Fouda, A.A. Nazeer and E.A. Ashour, Amino acids as environmentally-friendly corrosion inhibitors for Cu10Ni alloy in sulfide-polluted salt water: Experimental and theoretical study, *Zaštita Materijala*, 2011, **52**, 21–34.

8. S.A. Umoren, I.B. Obot, E.E. Ebenso and N.O. Obi-Egbedi, The Inhibition of aluminium corrosion in hydrochloric acid solution by exudate gum from Raphia hookeri, *Desalination*, 2009, **247**, 561–572. doi: 10.1016/j.desal.2008.09.005

9. M. Lebrini, F. Robert, P.A. Blandinières and C. Roos, Corrosion inhibition by *Isertia coccinea* plant extract in hydrochloric acid solution, *Int. J. Electrochem. Sci.*, 2011, **6**, 2443–2460. doi: 10.1016/S1452-3981(23)18196-X

10. P.C. Okafor, E.E. Ebenso and U.J. Ekpe, *Azadirachta indica* extracts as corrosion inhibitor for mild steel in acid medium, *Int. J. Electrochem. Sci.*, 2010, **5**, 978–993. doi: 10.1016/S1452-3981(23)15337-5

11. A. Toghan, H.S. Gadow, H.M. Dardeer and H.M. Elabbasy, New promising halogenated cyclic imides derivatives as potential corrosion inhibitors for carbon steel in hydrochloric acid solution, *J. Mol. Liq.*, 2021, **325**, 115136. doi: 10.1016/j.molliq.2020.115136

12. S.K. Singh, A.K. Mukherjee and M.M. Singh, Corrosion behaviour of mild steel in aqueous acetic acid solutions containing different amounts of formic acid, *Indian J. Chem. Technol.*, 2011, 18, 291–300. ID: 201202249851972426

13. M. Sivaraju and K. Kannan, Inhibitive properties of plant extract (Acalypha indica L.) on mild steel corrosion in 1 N phosphoric acid., *Int. J. ChemTech Res.*, 2010, **2**, no. 2, 1243–1253.

14. P.A.P. Idowu and F.O.S. Isaac, Environmental Failure of 2 M Acid Strength on Zinc Electroplated Mild Steel in the Presence of Nicotioana Tobacum, *Int. J. Electrochem. Sci.*, 2011, **6**, 4798–4810.

15. A.A. El-Meligi, Corrosion preventive strategies as a crucial need for decreasing environmental pollution and saving economics, *Recent Pat. Corros. Sci.*, 2010, **2**, 22–33. doi: 10.2174/1877610801002010022

16. J.T. Nwabanne and V.N. Okafor, Inhibition of the corrosion of mild steel in acidic medium by Vernonia amygdalina: adsorption and thermodynamics study, *J. Emerg. Trends Eng. Appl. Sci.*, 2011, **2**, 619–625.

17. C. Anushia, P. Sampathkumar and L. Ramkumar, Antibacterial and antioxidant activities in Cassia auriculata, *Glob. J. Pharmacol.*, 2009, **3**, 127–130.

18. L. Pari and M. Latha, Effect of Cassia auriculata flowers on blood sugar levels, serum and tissue lipids in streptozotocin diabetic rats, *Singapore Med. J.*, 2002, **43**, 617–621.

19. M.F. Ahmed, H. Thayyil, A.S. Rasheed and M. Ibrahim, Anti-ulcer activity of *cassia auriculata* leaf extract, *Pharmacogn. J.*, 2010, **2**, no. 16, 53–57. doi: 10.1016/S0975-3575(10)80050-1

20. S.A. Gaikwad, A.A. Kale, B.G. Jadhav, N.R. Deshpande and J.P. Salvekar, Anthelmintic activity of *Cassia auriculata L.* extracts – in vitro study, *J. Nat. Prod. Plant Resour.*, 2011, **1**, 62–66.

21. J.F.S. Ferreira, D.L. Luthria, T. Sasaki and A. Heyerick, Flavonoids from Artemisia annua L. as antioxidants and their potential synergism with artemisinin against malaria and cancer, *Molecules*, 2010, **15**, 3135–3170. doi: 10.3390/molecules15053135

22. M. Ramesh and L. Rajeshkumar, Case-studies on green corrosion inhibitors, *Sustainable Corrosion Inhibitors*, 2021, **107**, 204–221. doi: 10.21741/9781644901496-9

23. I. Pradipta, D. Kong and J.B.L. Tan, Natural organic antioxidants from green tea inhibit corrosion of steel reinforcing bars embedded in mortar, *Constr. Build. Mater.*, 2019, **227**, 117058. doi: 10.1016/j.conbuildmat.2019.117058

24. W. Emori, R.-H. Zhang, P.C. Okafor, X.-W. Zheng, T. He, K. Wei, X.-Z. Lin and C.-R. Cheng, Adsorption and corrosion inhibition performance of multi-phytoconstituents from *Dioscorea septemloba* on carbon steel in acidic media: Characterization, experimental and theoretical studies, *Colloids Surf. A*, 2020, **590**, 124534. doi: 10.1016/j.colsurfa.2020.124534

25. O.A. Akinbulumo, O.J. Odejobi and E.L. Odekanle, Thermodynamics and adsorption study of the corrosion inhibition of mild steel by *Euphorbia heterophylla L.* extract in 1.5 M HCl, *Results Mater.*, 2020, **5**, 100074. doi: 10.1016/j.rinma.2020.100074

26. C.K. Anyiam, O. Ogbobe, E.E. Oguzie, I.C. Madufor, S.C. Nwanonenyi, G.C. Onuegbu, H.C. Obasi and M.A. Chidiebere, Corrosion inhibition of galvanized steel in hydrochloric acid medium by a physically modified starch, *SN Appl. Sci.*, 2020, **2**, 520. doi: 10.1007/s42452-020-2322-2

27. A.I. Mohammed, M.M. Solomon, K. Haruna, S.A. Umoren and T.A. Saleh, Evaluation of the corrosion inhibition efficacy of *Cola acuminata* extract for low carbon steel in simulated acid pickling environment, *Environ. Sci. Pollut. Res.*, 2020, **27**, 34270–34288. doi: 10.1007/s11356-020-09636-w

28. R.T. Loto, Evaluation of the corrosion inhibition effect of the combined admixture of rosemary and cinnamon cassia oil on mild steel in weak acid electrolyte, *Sustainable Chem. Pharm.*, 2020, **17**, 100298. doi: 10.1016/j.scp.2020.100298

29. Y. Wu, Y. Zhang, Y. Jiang, Y. Qian, X. Guo, L. Wang and J. Zhang, Orange peel extracts as biodegradable corrosion inhibitor for magnesium alloy in NaCl solution: Experimental and theoretical studies, *J. Taiwan Inst. Chem. Eng.*, 2020, **115**, 35–46. doi: https://doi.org/10.1016/j.jtice.2020.10.010

30. I. Dhouibi, F. Masmoudi, M. Bouaziz and M. Masmoudi, A study of the anti-corrosive effects of essential oils of rosemary and myrtle for copper corrosion in chloride media, *Arabian J. Chem.*, 2020, **14**, no. 2, 102961. doi: 10.1016/j.arabjc.2020.102961

31. N. Al Otaibi and H.H. Hammud, Corrosion Inhibition Using Harmal Leaf Extract as an Eco-Friendly Corrosion Inhibitor, *Molecules*, 2021, **26**, 7024. doi: 10.3390/molecules26227024

32. M. Tanga, S. Deng, J. Xua, D. Xu, D. Shaoa, G. Du and X. Lia, A comparison of the corrosion inhibition on 1060 aluminum in HCl solution between water and alcoholic extracts of *Mikania micrantha*, *Corros. Sci*., 2024, **228**, 111799. doi: 10.1016/j.corsci.2023.111799

33. E.E. Mbamalu and A.P. Chinedu, Assessment of the Corrosion Inhibitory Potentials of *Chromolaena Odorata* Leaf Extract on Mild Steel in Hydrogen Chloride Acid, *Mor. J. Chem*., 2023, **14**, 188–204. doi: 10.48317/IMIST.PRSM/morjchem-v10i3.30521

34. M. Lebrini, F. Robert, A. Lecante and C. Roos, Corrosion inhibition of C38 steel in 1 M hydrochloric acid medium by alkaloids extract from *Oxandra asbeckii* plant, *Corros. Sci*., 2011, **53**, 687–695. doi: 10.1016/j.corsci.2010.10.006

35. A.S. Fouda, S.E.H. Etaiw, A.M. Ibrahim and A.A. El-Hossiany, Insights into the use of two novel supramolecular compounds as corrosion inhibitors for stainless steel in a chloride environment: experimental as well as theoretical investigation, *RSC Adv*., 2023, **13**, 35305–35320. doi: 10.1039/D3RA07397A

36. A.-R.I. Mohammed, M.M. Solomon, K. Haruna, S.A. Umoren and T.A. Saleh, Evaluation of the corrosion inhibition efficacy of *Cola acuminata* extract for low carbon steel in simulated acid pickling environment, *Environ. Sci. Pollut. Res*., 2020, **27**, 34270–34288. doi: 10.1007/s11356-020-09636-w

37. R.T. Loto, Evaluation of the corrosion inhibition effect of the combined admixture of rosemary and cinnamon cassia oil on mild steel in weak acid electrolyte, *Sustainable Chem. Pharm*., 2020, **17**, 100298. doi: 10.1016/j.scp.2020.100298

38. S.L.A. Kumar, P. Iniyavan, M.S. Kumar and A. Sreekanth, Corrosion inhibition studies of *Ecbolium viride* extracts on mild steel in HCl, *J. Mater. Environ. Sci*., 2012, **3**, 461–468.

39. S. Jyothi and K. Rathidevi, Experimental and theoretical investigation on corrosion inhibition of mild steel in sulphuric acid by *Coccinia indica* leaves extract, *Rasāyan J. Chem*., 2017, **10**, 1253–1260. doi: 10.7324/RJC.2017.1041924

40. E. Khamis, The effect of temperature on the acidic dissolution of steel in the presence of inhibitors, *Corrosion*, 1990, **46**, 476–484. doi: 10.5006/1.3585135

41. A.Y. El-Etre, Inhibition of acid corrosion of carbon steel using aqueous extract of olive leaves, *J. Colloid Interface Sci*., 2007, **314**, 578–583. doi: 10.1016/j.jcis.2007.05.077

42. M.T.G. de Sampaio, C.M. Fernandes, G.G.P. de Souza, E.S. Carvalho, J.A.C. Velasco, J.C.M. Silva, O.C. Alves and E.A. Ponzio, Evaluation of Aqueous Extract of *Mandevilla fragrans* Leaves as Environmental-Friendly Corrosion Inhibitor for Mild Steel in Acid Medium, *J. Bio Tribo Corros*., 2021, **7**, 14. doi: 10.1007/s40735-020-00445-9

43. A.S. Fouda, H.M. Abdel-Wahed, M.F. Atia and A. El-Hossiany, Novel porphyrin derivatives as corrosion inhibitors for stainless steel 304 in acidic environment: synthesis, electrochemical and quantum calculation studies, *Sci. Rep*., 2023, **13**, 17593. doi: 10.1038/s41598-023-44873-2

44. M. Lebrini, F. Robert and C. Roos, Alkaloids extract from *Palicourea guianensis* plant as corrosion inhibitor for C38 steel in 1 M hydrochloric acid medium, *Int. J. Electrochem. Sci.*, 2011, **6**, 847–859.

45. W.A. Badawy, F.M. Al-Kharafi and A.S. El-Azab, Electrochemical behaviour and corrosion inhibition of Al, Al-6061 and Al–Cu in neutral aqueous solutions, *Corros. Sci.*, 1999, **41**, 709–727. doi: 10.1016/S0010-938X(98)00145-0

46. I. Ahamad, R. Prasad and M.A. Quraishi, Adsorption and inhibitive properties of some new Mannich bases of Isatin derivatives on corrosion of mild steel in acidic media, *Corros. Sci.*, 2010, **52**, 1472–1481. doi: 10.1016/j.corsci.2010.01.015

47. E. Peñaloza, C. Holandino, C. Scherr, P.I.P. de Araujo, R.M. Borges, K. Urech, S. Baumgartner and R. Garrett, Comprehensive metabolome analysis of fermented aqueous extracts of Viscum album L. by liquid chromatography– high resolution tandem mass spectrometry, *Molecules*, 2020, **25**, 4006. doi: 10.3390/molecules25174006

48. L.A. Nnanna, I.O. Owate, O.C. Nwadiuko, N.D. Ekekwe and W.J. Oji, Adsorption and corrosion inhibtion of Gnetum africana leaves extract on carbon steel, *Int. J. Mater. Chem.*, 2013, **3**, 10–16. doi: 10.5923/j.ijmc.20130301.03

49. G.N. Mu, X. Li and F. Li, Synergistic inhibition between o-phenanthroline and chloride ion on cold rolled steel corrosion in phosphoric acid, *Mater. Chem. Phys.*, 2004, **86**, 59–68. doi: 10.1016/j.matchemphys.2004.01.041

50. E.B. Agbaffa, E.O. Akintemi, E.A. Uduak and O.E. Oyeneyin, Corrosion inhibition potential of the methanolic crude extract of Mimosa pudica leaves for mild steel in 1 M hydrochloric acid solution by weight loss method, *Sci. Lett.*, 2021, **15**, 23–42. doi: 10.24191/sl.v15i1.11791

51. M. Eissa, S.H. Etaiw, E.E. El-Waseef, A. El-Hossiany and A.S. Fouda, The impact of environmentally friendly supramolecular coordination polymers as carbon steel corrosion inhibitors in HCl solution: synthesis and characterization, *Sci. Rep.*, 2024, **14**, 2413. doi: 10.1038/s41598-024-51576-9

52. A.S. Fouda, S.A. Abd El-Maksoud, A. El-Hossiany and A. Ibrahim, Corrosion protection of stainless steel 201 in acidic media using novel hydrazine derivatives as corrosion inhibitors, *Int. J. Electrochem. Sci.*, 2019, **14**, 2187–2207. doi: 10.20964/2019.03.15

53. N. Raghavendra, L.V. Hublikar, S.M. Patil, P.J. Ganiger and A.S. Bhinge, Efficiency of sapota leaf extract against aluminium corrosion in a 3 M sodium hydroxide hostile fluid atmosphere: a green and sustainable approach, *Bull. Mater. Sci.*, 2019, **42**, 226. doi: 10.1007/s12034-019-1922-1

54. A.S. Fouda, S.H. Etaiw, D.M. Abd El-Aziz, A.A. El-Hossiany and U.A. Elbaz, Experimental and theoretical studies of the efficiency of metal–organic frameworks (MOFs) in preventing aluminum corrosion in hydrochloric acid solution, *BMC Chem.*, 2024, **18**, 21. doi: 10.1186/s13065-024-01121-6

55. A.S. Fouda, S.A. Abd El-Maksoud, A.A.M. Belal, A. El-Hossiany and A. Ibrahium, Effectiveness of some organic compounds as corrosion inhibitors for stainless steel 201 in 1M HCl: experimental and theoretical studies, *Int. J. Electrochem. Sci.*, 2018, **13**, 9826–9846. doi: [10.20964/2018.10.36](10.20964/2018.10.36)

56. A.S. Fouda, S.M.A. Motaal, A.S. Ahmed, H.B. Sallam, A. Ezzat and A. El-Hossiany, Corrosion Protection of Carbon Steel in 2 M HCl Using Aizoon canariense Extract, *Biointerface Res. Appl. Chem.*, 2022, **12**, 230–243. doi: 10.33263/BRIAC121.230243

57. A.S. Fouda, M.A. Azeem, S. Mohamed and A. El-Desouky, Corrosion inhibition and adsorption behavior of nerium oleander extract on carbon steel in hydrochloric acid solution, *Int. J/ Electrochem. Sci.*, 2019, **14**, 3932–3948. doi: [10.20964/2019.04.44](10.20964/2019.04.44)

58. W.J. Lorenz and F. Mansfeld, Determination of corrosion rates by electrochemical DC and AC methods, *Corros. Sci.*, 1981, **21**, 647–672. doi: [10.1016/0010-938X(81)90015-9](10.1016/0010-938X(81)90015-9)

59. S. Zhang, L. Hou, H. Du, H. Wei, B. Liu and Y. Wei, A study on the interaction between chloride ions and CO2 towards carbon steel corrosion, *Corros. Sci.*, 2020, **167**, 108531. doi: [10.1016/j.corsci. 2020.108531](10.1016/j.corsci.2020.108531)

60. A.S. Fouda, A. El-Mekabaty, I.E.I. Shaaban and A. El-Hossiany, Synthesis and Biological Evaluation of Novel Thiophene Derivatives as Green Inhibitors for Aluminum Corrosion in Acidic Media, *Prot. Met. Phys. Chem. Surf.*, 2021, **57**, 1060–1075. doi: [10.1134/S2070205121050075](10.1134/S2070205121050075)

61. A.S. Fouda, S. Rashwan, A. El-Hossiany and F.E. El-Morsy, Corrosion Inhibition of Zinc in Hydrochloric Acid Solution Using Some Organic Compounds as Eco-Friendly Inhibitors, *J. Chem. Biol. Phys. Sci.*, 2019, **9**, 1–24.

62. M.A. Khaled, M.A. Ismail, A.A. El-Hossiany and A.S. Fouda, Novel pyrimidine-bichalcophene derivatives as corrosion inhibitors for copper in 1 M nitric acid solution, *RSC Adv.*, 2021, **11**, 25314–25333. doi: [10.1039/D1RA03603C](10.1039/D1RA03603C)

63. M.M. Motawea, A. El-Hossiany and A.S. Fouda, Corrosion control of copper in nitric acid solution using chenopodium extract, *Int. J. Electrochem. Sci.*, 2019, **14**, 1372–1387. doi: [10.20964/2019.02.29](10.20964/2019.02.29)

64. N. Soltani, N. Tavakkoli, A. Attaran, B. Karimi and M. Khayatkashani, Inhibitory effect of Pistacia khinjuk aerial part extract for carbon steel corrosion in sulfuric acid and hydrochloric acid solutions, *Chem. Pap.*, 2020, **74**, 1799–1815. doi: [10.1007/s11696-019-01026-y](10.1007/s11696-019-01026-y)

65. R. Haldhar, D. Prasad and N. Bhardwaj, Extraction and experimental studies of Citrus aurantifolia as an economical and green corrosion inhibitor for mild steel in acidic media, *J. Adhes. Sci. Technol.*, 2019, **33**, 1169–1183. doi: [10.1080/01694243.2019.1585030](10.1080/01694243.2019.1585030)

66. A.S. Fouda, S.A. Abd El-Maksoud, A. El-Hossiany and A. Ibrahim, Evolution of the corrosion-inhibiting efficiency of novel hydrazine derivatives against corrosion of stainless steel 201 in acidic medium, *Int. J. Electrochem. Sci.*, 2019, **14**, 6045–6064. doi: [10.20964/2019.07.65](10.20964/2019.07.65)

67. A. Yurt, B. Duran and H. Dal, An experimental and theoretical investigation on adsorption properties of some diphenolic Schiff bases as corrosion inhibitors at acidic solution/mild steel interface, *Arab. J. Chem.*, 2014, **7**, 732–740. doi: 10.1016/j.arabjc.2010.12.010

68. A. Biswas, S. Pal and G. Udayabhanu, Experimental and theoretical studies of xanthan gum and its graft co-polymer as corrosion inhibitor for mild steel in 15% HCl, *Appl. Surf. Sci.*, 2015, **353**, 173–183. doi: 10.1016/j.apsusc.2015.06.128

69. M. Benahmed, N. Djeddi, S. Akkal and H. Laouar, Saccocalyx satureioides as corrosion inhibitor for carbon steel in acid solution, *Int. J. Ind. Chem.*, 2016, **7**, 109–120. doi: 10.1007/s40090-016-0082-z

70. S. Deng and X. Li, Inhibition by Ginkgo leaves extract of the corrosion of steel in HCl and H_2SO_4 solutions, *Corros. Sci.*, 2012, **55**, 407–415. doi: 10.1016/j.corsci.2011.11.005

♦ ♦ ♦